Detection of Error Correlates in the Motor Cortex in a Long Term Clinical Trial of ECoG based Brain Computer Interface

Vincent Rouanne[1][a], Maciej Śliwowski[1,2][b], Thomas Costecalde[1][c], Alim Louis Benabid[1,3][d]
and Tetiana Aksenova[1][e]

[1]Univ. Grenoble Alpes, CEA, LETI, Clinatec, F-38000 Grenoble, France
[2]CEA, LIST, Gif-sur-Yvette, France
[3]CHU Grenoble Alpes, Grenoble, France

Keywords: Brain Computer Interface, Error Correlates, Sensory-motor Cortex, Machine Learning, Clinical Trial, Tetraplegic Subject.

Abstract: Error correlates are thought to be promising for BCIs as a way to perform error correction or prevention, or to label data in order to perform online adaptation of BCIs' control models. Current state-of-the-art BCIs are motor-imagery-based invasive BCIs and thus have no access to neural data apart from sensory-motor cortices. We investigated at the single trial level the presence and detectability of error correlates in the primary motor cortex during observation or motor imagery (MI) control of a BCI with two discrete classes by a tetraplegic user. We show that error correlates can be detected using a broad range of classifiers, namely Support Vector Machine (SVM), logistic regression, N-way Partial Least Squares (NPLS), Multilayer Perceptron (MLP) and Convolutional Neural Network (CNN) with respective mean AUC of the ROC curve of 0.645, 0.662, 0.642, 0.680 and 0.630 in the observation condition, and 0.623, 0.605, 0.603, 0.626 and 0.580 in the MI-control condition. We also suggest that these error correlates are stable in time. These findings suggest that error correlates could be used in clinical trials using invasive motor-imagery-based BCIs for error correction or prevention.

1 INTRODUCTION

Brain computer interfaces (BCI) are promising tools that use neural signal recordings to directly control effectors. However, BCIs are currently mostly used in research laboratories due to several limitations, including their often too low performances and their requirement to be calibrated in specific conditions with the assistance of a researcher. Both of these issues can be alleviated using a biomimetic strategy of learning for the training of the decoder of the BCI. In humans, brain signals that generate correct actions can be reinforced, while action recognized as erroneous can be corrected and may have also reduced probability of being performed in the future. This learning requires feedback in order to know if a given action was correct or erroneous. In the case of

an action performed by a human controlled BCI, the human receives feedback (e.g. visual) regarding the success of the action, whereas the machine does not. Having the user consciously (e.g. orally or physically) transferring this feedback to the BCI may be tiring, impractical or even impossible depending on the condition of the user. However, the feedback received by the user may produce specific brain activity. A BCI able to detect such brain activity would thus have access to learning-enabling feedback. Brain activity correlated to errors was recorded as early as 1991 in the experiments of Falkenstein et al. (1991). Detection of error correlates during BCI operation can provide a way to either correct mistakes after they have been performed or train or update the models used to control the BCI (Chavarriaga, Sobolewski, & Millan, 2014). The ability to reliably detect error

---

[a] https://orcid.org/0000-0001-7708-8176
[b] https://orcid.org/0000-0001-6744-1714
[c] https://orcid.org/0000-0003-2216-4447
[d] https://orcid.org/0000-0002-4479-1807
[e] https://orcid.org/0000-0003-4007-2343

correlates in brain signals is thus valuable for the development of BCIs.

Although error correlates can be used directly as control signals to operate a BCI (Chavarriaga, Iturrate, & Millan, 2016), we are interested here in their use as a secondary signal acquired to improve the performance of BCIs. Notably, error correlates have been used in simulations and online experiments to automatically correct errors during BCI operation (Even-Chen et al., 2018; Parra, Spence, Gerson, & Sajda, 2003) or to update control models without the use of new externally labeled data (Blumberg et al., 2007; Spüler, Rosenstiel, & Bogdan, 2012).

The error correlate discovered by Falkenstein et al. (1991) is the error-related signal mostly used in BCI applications. This waveform called the error-related potential (ErrP) is composed of a negative potential deflection over the fronto-central scalp area roughly 50 to 100ms after the event that induced it, followed by a centro-parietal positive deflection (Chavarriaga, Sobolewski, & Millan, 2014). Conveniently for BCI, ErrPs are relatively stable across time and tasks (Chavarriaga & Millan, 2010; Ferrez & del R. Millan, 2008), are elicited when an error is performed by a BCI controlled or observed by a user (Ferrez & del R. Millan, 2008; Schalk, Wolpaw, McFarland, & Pfurtscheller, 2000) and are detectable at the single-trial level (Parra, Spence, Gerson, & Sajda, 2003). However, the localization of these ErrPs is a drawback for current state-of-the-art BCIs. The BCIs best in terms of performance are invasive and thus often have access to limited recording areas over or in the brain (Benabid et al., 2019; Wodlinger et al., 2014). The primary sensory-motor cortex is the best candidate for the recording area of an invasive BCI due to its ability to generate motor imagery signals. In such circumstances, ErrPs cannot be recorded when using these BCIs. We focus hereafter on the specific case of BCIs that acquire brain signals from the sensory-motor cortex only.

ErrPs are not the only error correlates that can be recorded from brain signals. Error correlates have been reported in the primary motor and somatosensory cortex. In a MEG study, Koelewijn et al. (2008) reported a stronger beta rebound after an outcome error than after a correct task outcome, both when observing or performing a motor task. Previous work by van Schie et al. (2004) demonstrated the existence of error correlates in the motor cortex by showcasing the variability of the lateralized readiness potential between correct and erroneous response in an Eriksen flanker task. Although their experiment was performed on non-human primates and using intracortical electrodes, Inoue et al. (2016)

successfully showed that end-point errors during reaching tasks are encoded in the primary motor cortex. Maybe more importantly, they provided evidence that these error signals are necessary for adaptation in reaching movements. In an EEG-ECoG combined study, Völker et al. (2018) showed that error processing in the human brain involved modulation of brain activity in the high gamma frequency band (60-90Hz), including modulations in the precentral gyrus and post central gyrus. These findings are consistent with the more recent study by Wilson et al. (2019), in which they also found an increase in the high gamma frequency band (70-100Hz) after erroneous BCI task outcomes with respect to correct ones. Finally, Milekovic et al. (2012, 2013) reported detection of errors at the single trial-level using ECoG in the motor region (accuracy≥76%) during motor execution by able-bodied subjects. Apart from Milekovic et al., no single-trial detection of error correlates in the motor cortex have been reported. However, Milekovic et al.'s studies have the drawbacks of being performed with overt movement tasks instead of BCI operation by tetraplegic user with motor imagery. Additionally, these studies were performed with subjects implanted with large ECoG grids due to intractable epilepsy. Although they report detectability using electrodes located over the motor cortex, this does not insure the detectability using electrodes positioned with motor imagery for BCI in mind.

In this study, we perform an experiment where a tetraplegic user receives erroneous feedback from a BCI while observing or controlling its actions. Neural data are acquired using chronic ECoG implants located over the left and right primary sensory-motor cortex. The BCI is controlled using motor imagery and errors should be detected on a single trial basis using the brain data recorded from the motor cortex. Several decoding models are trained for the purpose of detecting error correlates.

2 METHODS

2.1 Data Recording

The subject in this experiment was a 28-year-old male who had tetraplegia following a C4-C5 spinal cord injury (ASIA scale levels of the subject are presented in Benabid et al. (2019)). The subject was implanted with two WIMAGINE (Mestais et al., 2015) ECoG implants 24 months prior to the experiments in this study, as a participant in the clinical trial "BCI and Tetraplegia". The "BCI and Tetraplegia" clinical trial
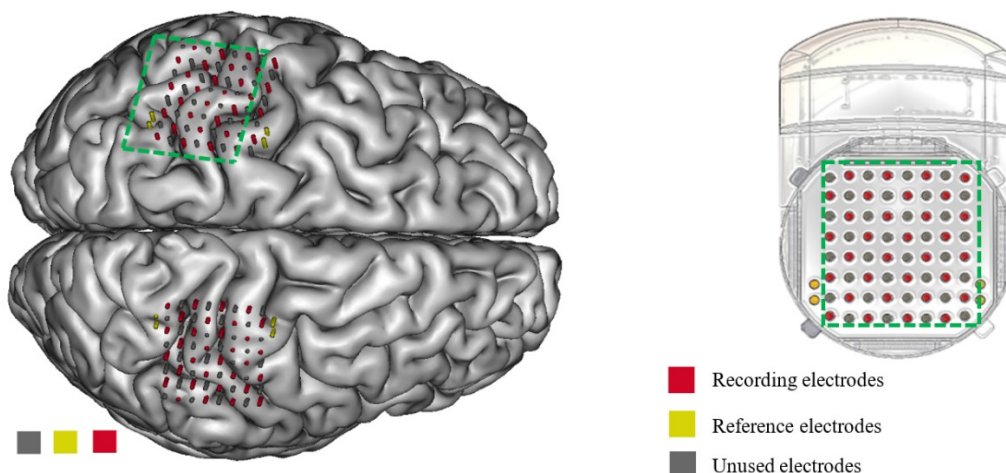
Figure 1: A. Position of the electrodes of each WIMAGINE implant over the right and left sensory-motor areas on a reconstruction of the subject's brain from MRI. B. Schematic view of a WIMAGINE implant.

(ClinicalTrials.gov identifier: NCT02550522) was approved by French authorities: Agence nationale de sécurité du médicament et des produits de santé (ANSM) with the registration Number: 2015-A00650-49 and the ethical committee (Comité de Protection des Personnes - CPP) with the Registration number: 15-CHUG-19. The implants were positioned over the left and right sensory-motor cortex (Figure 1). Experimental data was recorded at a sampling rate of 586Hz from 32 out of the 64 electrodes of each implant because of limited data rates.

2.2 Experimental Setup

The subject was sited in front of a computer screen where a human avatar was represented from a third person perspective. An instruction panel that either displayed a GO or STOP label was also displayed (Figure 2). The avatar could either stand still or walk forward at a fixed speed. Two conditions of control were designed. In the first condition (condition 1), the subject had no control over the avatar, which was controlled by the computer. In the second condition (condition 2), the avatar was controlled by the subject using leg motor imagery. The subject was already trained to control a similar avatar using leg motor imagery prior to this experiment (Benabid et al., 2019).

In condition 1, the subject was instructed to focus on the avatar and to expect the avatar to follow the instructions displayed on the instruction panel as if he was controlling the avatar's actions through motor imagery. In this condition, the instruction panel switched its instruction every 5 to 15 seconds. The
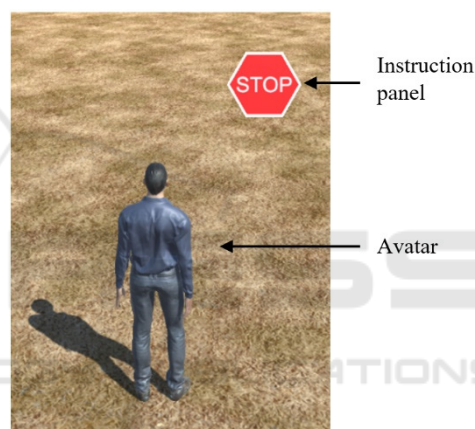

Figure 2: The environment is similar to the one in Benabid et al. (2019). The subject either watched the avatar move automatically (condition 1), or controlled it using leg motor imagery (condition 2). When the instruction panel showed "STOP" the avatar was supposed to stay idle, whereas when it showed "GO" the avatar was supposed to walk.

avatar followed the change in instruction with a random reaction speed between 200ms and 500ms. Additionally, error periods were automatically introduced in this condition. During error periods, the avatar switched its state to the opposite of the one required from the instruction panel. Error and correct periods always lasted at least two seconds, and error periods never lasted more than three seconds. Error periods were introduced at random following the previous restrictions with an error rate of approximately two to three errors per minute. Nineteen sessions of eleven minutes of recording were acquired over 268 days in condition 1.

In condition 2, the subject controlled the avatar using leg motor imagery. Walking was triggered by

performing both legs motor imagery, while standing still was performed by not performing motor imagery. In this condition, the duration of error and correct periods as well as the error rate were entirely determined by the control of the subject over the BCI. Since the subject was already trained for such a task and had achieved high control of the BCI, a new control model was built specifically for the experiment using a purposely-reduced dataset as training set. This was performed in order to ensure that errors would still occur in this simple control paradigm. Thirteen sessions of on average eleven minutes of recording were acquired over 141 days in condition 2.

Condition 1 was designed to ensure that error correlates could be recorded in the motor cortex with the present electrode setup, without any interference from motor imagery signals. It also ensured that error correlates detected in condition 2 were not due to motor imagery confounds. Condition 2 was designed to assess if error correlates could be detected while the BCI was used.

2.3 Data Labelling

In both conditions, the goal of the experiment was to distinguish correct from erroneous events. Events were defined as moments when the avatar changes its state. Specifically, correct events were defined as the avatar changing its state to the one required by the instruction panel, and error events were defined as the avatar changing its state to the opposite of the one required by the instruction panel. We expected error correlates to appear after such erroneous events, as was the case in Milekovic et al. (2013).

Epochs of one second and spaced by 100ms (90% overlap) were considered for the classification of correct or erroneous events. The first six full epochs after an event were labeled according to the event type. The first such epoch contained temporal data from the event onset to one second after the event. The last epoch contained temporal data from 0.5s after the event to 1.5s after the event (Figure 3). Additionally, epochs that were too close to another event were discarded. The inclusion of several epochs for each event was performed with two goals in mind. The first one is to counterbalance the issue of synchronization. Indeed the timing of the brain response to the erroneous or correct events may vary depending on several conditions, such as the attention level, the tiredness of the subject, or the workload as is the case in classical ErrPs paradigms (Iturrate, Chavarriaga, Montesano, Minguez, & Millán, 2012). Additionally, there was some jitter in the reaction
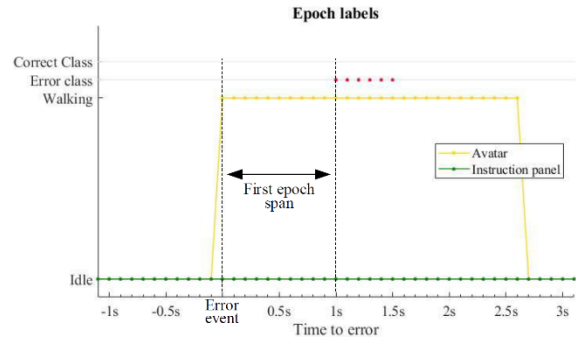

Figure 3: Example of an error event where the avatar starts walking when it is supposed to stay idle. Red dots indicate epochs belonging to the error class. The first epoch included contains neural data from the onset of the error to one second after.

time of the avatar itself to a change of command (e.g. the avatar must finish a step before stopping), which was estimated to be up to 300ms. Adding several epochs for each event increased the probability of having the desired brain signal in one of them at the cost of some label uncertainty.

2.4 Feature Extraction

Time-frequency decomposition of brain signals is classically performed in the literature for the detection of error correlates in the motor cortex (Milekovic, Ball, Schulze-Bonhage, Aertsen, & Mehring, 2012; Wilson et al., 2019). Therefore, time-frequency information was extracted for each 1s epoch and for the 64 electrodes. Continuous complex wavelet transform was applied using a family of fifteen Morlet wavelets of central frequencies from 10Hz to 150Hz. For each 1s epoch, the absolute value of this time-frequency data was averaged over the temporal dimension into ten non-overlapping windows of 100ms. The resulting feature tensor for each epoch was thus of shape $10 \times 15 \times 64$, respectively along the temporal, frequential and spatial dimensions.

2.5 Data Balance

Due to the design of the experiment, there was an imbalance in the class repartition of the data in both condition 1 and 2 (Table 1). Additionally, error epochs and correct epochs could each be of two separate types. Error epochs could be due to the avatar starting to walk when expected to stand idle, or due to the avatar stopping when expected to walk. Similarly, correct epochs could be due to the avatar starting to walk when expected to walk or due to the

avatar stopping when expected to stop. The existence of these sub-classes could potentially create strong confounds for the error correlate detection if they were not balanced (e.g. a motor imagery confound in condition 2). The training dataset was balanced by oversampling the three sub-classes with the least number of epochs to the same number of epochs as the most populated sub-class. Oversampling was performed by repetition of the epochs present in the sub-classes.

Table 1: Number of epoch in each class for each condition.

	Epoch type	Condition 1	Condition 2
Number of	Correct	7539	4412
epochs	Error	2307	3580

2.6 Decoders

Several decoder types were trained and compared on both condition 1 and 2. We trained classical decoders used in BCI studies, namely support vector machine (SVM), logistic regression, multilayer perceptron (MLP), convolutional neural networks (CNN) and N-way partial least squares (NPLS). These decoders share a characteristic of simplicity as the dataset in this problem is of high dimensionality (9600 input features), and with a relatively low amount of samples (~9000 and ~8000 in condition 1 and 2 respectively). For various example of use of these decoders for BCI, the interested reader may refer to Lotte et al. (2018).

2.6.1 SVM & Logistic Regression

SVM and logistic regression are considered as state-of-the-art methods for binary classification. These methods are most often used in combination with kernels, which can act as nonlinear projections of the input data into high dimensional spaces without having to specify the transformed input data. Regular kernels (Gaussian and polynomial) were not used as in preliminary studies they tended to strongly overfit the training datasets, even with strong regularization parameters and low Gaussian kernel scale (<10-5) or low polynomial kernel order (order of 2 or 3).

Since we have more features in our input dataset than sample points, regularization was used for both SVM and logistic regression. For both methods, ridge regularization was applied. After preliminary results, lambda was set to one.

2.6.2 NPLS

NPLS is a less known method in the field of BCIs. It is a linear method that is particularly suitable for tensor-based high dimensional datasets. It also has the advantage of being updatable using low computational power and without requiring to save the full original training dataset (Eliseyev et al., 2017).

2.6.3 MLP

MLP is a fully connected feedforward artificial neural network. It may be interpreted as a logistic regression model preceded by a nonlinear transformation which increases predictive power of the model. Proposed MLP model consisted of one hidden layer with 100 neurons (with learnable weights) followed by a ReLU activation. As all neurons are connected to each input component and produce linear combination of input features, it results in a huge number of parameters to train. Considering the size of the dataset and number of parameters we decided to regularize the model by applying batch normalization, dropout with probability of a neuron being zeroed 0.5, L2 regularization on model's weights with lambda equal 0.1 and early stopping on validation set.

2.6.4 CNN

CNNs take advantage of data structure. They are capable of capturing invariant patterns that may occur in different parts of the signal. They have less trainable parameters than similar MLP because of filters weight sharing which means that the same set of small filters is applied all over the data. We decided to use CNN as there is a possible shift in error correlates synchronization inside epochs. By sliding convolutional filter over the signal in the time domain we expected network to recognize error correlates (which we expect to be time invariant) occurring in different epoch's moment with the same filter. It results in lower number of parameters and possible higher performance in detecting time invariant patterns. Proposed CNN used 128 filters of shape $5 \times 15 \times 64$ respectively in time, frequency and channels dimension. Each filter was slid only over time dimension with stride equal 1. We applied the same regularization methods as for the MLP.

2.7 Decoder Application and Performance Evaluation

We report the performance of each model regarding the desired task, which is the detection of error or correct events. Up to 6 epochs were used for each event but the signal corresponding to an error may not be found in all of these epochs. Events were classified

as errors as soon as one of their associated epochs was classified as an error. The number of correct and error events in each fold are summarized in Table 2 and 3.

The performance of the event decoder was assessed over a five-fold cross-validation performed across sessions, which means that an equal number of sessions was presented in each of the five data splits. Each split was used as a testing fold once, with the corresponding other four splits used as training fold. The performance of each decoder was evaluated using the area under the curve (AUC) of the receiver operating characteristic (ROC) curve for each test fold of the cross-validation, for the task of event classification.

Table 2: Repartition of error and correct events in each fold for condition 1 (observation).

	Event type	Fold 1	Fold 2	Fold 3	Fold 4	Fold 5
Train	Correct	1006	992	985	981	1072
	Error	283	308	316	317	332
Test	Correct	253	267	274	278	187
	Error	106	81	73	72	57

Table 3: Repartition of error and correct events in each fold for condition 2 (control with motor imagery).

	Event type	Fold 1	Fold 2	Fold 3	Fold 4	Fold 5
Train	Correct	633	554	558	590	609
	Error	519	457	464	469	483
Test	Correct	103	182	178	146	127
	Error	79	141	134	129	115

3 RESULTS

In the first condition the avatar was not controlled by the subject and the subject monitored only the actions taken by the BCI. In the second condition the state of the avatar was controlled by the user through leg motor imagery. The results for each decoder and condition are summarized in Table 4 and Figure 4. A Friedman test was performed to compare model performances within each condition group. No significant differences was found between models in condition 1 (p-value = 0.13) or between models in condition 2 (p-value = 0.08).

The results we report show that MLP achieved the best performance in both the observation and MI-control conditions. CNN and MLP were the two models that allowed for the most complex representations, such as nonlinear relationships. Taking into account that regularization would limit the drawbacks associated to their high number of parameters, we expected these models to perform the

Table 4: Mean and standard deviation over five test folds of the area under the curve of the receiver operating characteristic curve for the classification of error vs correct events.

Condition 1	NPLS	Logistic	SVM	MLP	CNN
AUC mean	0.642	0.662	0.645	**0.680**	0.630
AUC std	0.096	0.106	0.119	0.131	0.124

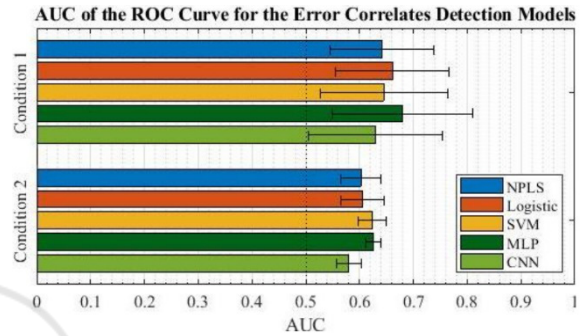| Condition 2	NPLS	Logistic	SVM	MLP	CNN
AUC mean	0.603	0.605	0.623	**0.626**	0.580
AUC std	0.037	0.040	0.027	0.014	0.022

Figure 4: Mean area under the curve of the receiver operating characteristic curve for each model and each condition. Error bars on the left and right of the mean each represent one time the standard deviation.

best. CNN had less parameters than MLP and was also more adapted to the task of re-synchronizing the error correlates. However, the performances of CNN models were the worst across all decoders. A possible explanation for this is that both neural network architectures (and neural networks in general) had a high number of hyperparameters and we did not perform an exhaustive search of these hyperparameter spaces (e.g. learning rate, number of filters, regularization weight).

In each condition, the three other decoders performed similarly, with small variabilities demonstrating better performances for logistic regression in the first condition and for SVM in the second condition. NPLS always performed slightly worse than SVM and logistic regression.

Performance across different folds was represented by the standard deviation of the AUC. Since cross-validation was performed session-wise, this standard deviation can be used to predict the generalization capabilities of each model over different datasets. In the observation condition, the standard deviations of the AUC for each decoder were close to one another, with NPLS having the lowest. In the MI-control condition MLP had the lowest standard deviation, close to twice lower than the standard deviation of other decoders.

On average, the AUC of the decoders in condition 1 decreased by 6.8% for condition 2. This was expected since the motor imagery signals used to control the BCI in the MI-control condition can be regarded as noise for the classification of error and correct events. However, the standard deviation of the AUC was up to ten times larger in the observation condition than in the MI-control condition. We suggest that the higher variability in the observation condition was due to a higher variability in the attention level of the subject than in the MI-control condition. Indeed, in the MI-control condition the subject was more engaged in the task since he had active control over the avatar's actions. In the observation condition, the subject was more vulnerable to distractions due to the lack of interaction required by the condition. We hypothesize that the attention level modulated the strength of the error correlates in the motor cortex, similarly to how it modulates classical ErrPs (Yeung, Holroyd, & Cohen, 2005).

4 DISCUSSION

4.1 Impact of Event Latency

We hypothesize that the error correlate reported here could be modulated by the length of correct or error periods prior to an event. Although the duration of these periods, or latency before each event, was partly controlled in condition 1 there was no inclusion or exclusion criterion based on it in condition 2. We suggest that this latency may influence the brain response to events. For example, correct events after a long erroneous period may elicit a stronger brain response than after a short erroneous period. Due to the relatively small dataset acquired in this experiment, separating the events based on latency was not possible, but larger studies should take it into account when possible.

4.2 Inter-session Stability of Error Correlates

It should be noted that the different sessions of this experiment were recorded over the course of several months. The cross-validation was performed session-wise, which means that the models were partly trained on data recorded far away temporally from the data they were tested on. This leads us to suggest that the error correlates we report in the motor cortex may exhibit a certain temporal stability, similarly to ErrPs.

4.3 Single Trial Detection of Error Correlates

Although the AUCs reported in this study are not considerably high, these are still above chance levels for each algorithm tested here. We therefore suggest that there effectively is an error correlate detectable at the single trial level in the motor cortex when either observing or controlling a BCI that performed an erroneous action. Additionally, although the AUC decreased between the observation and MI-control condition, the ability to detect error correlates in the motor cortex during operation of the BCI using motor imagery is valuable not only from a neuroscience perspective where it could provide some additional insight on the motor learning mechanisms, but also for potential applications in state-of-the-art BCIs for which it is a requirement.

4.4 Decoders for Online BCIs

Although SVM, logistic regression and neural networks are recognized as powerful methods, it is not easy to update these classifier online without retraining them on the full training dataset. This property can be a drawback for some BCI applications, including online training which is considered as better than classical training with feedback that is not generated by the control of the BCI. More investigation would be required if these decoders were to be trained or updated in online BCI paradigms. In such cases, one should preferably use NPLS over these decoders, as NPLS demonstrated only slightly lower performances (up to 3.7% lower) than the other decoders while being easily trainable and updatable online.

5 CONCLUSION

Like previous independent studies reported, we found error correlates in the time-frequency decomposition of brain signals recorded in the sensory-motor cortex using ECoG. However, to our knowledge this study is the first to report the possibility to detect at the single-trial-level error correlates in the sensory-motor cortex during operation of a BCI. This study is also the first one to report error correlates in the sensory-motor cortex of a tetraplegic subject. Additionally, in this study the operation of the BCI is performed using motor imagery, further highlighting the value of these results since a BCI with access to neural data from the motor cortex only (such as invasive state-of-the-art motor-imagery-based BCIs) could still be able to

detect error correlates and potentially use them for error correction or model adaptation. The fact that the detection accuracy of the NPLS was close to other model is also a strong point for potential online model adaptations, as it is computationally fast to update in real time compared to the other models presented.

The main limitation of this study is that it was restricted to the first subject of the clinical trial. However, this clinical trial is expected to have a total of 5 subjects, who could later be added to this study. Other perspective future studies include implementing automatic error correction for this binary BCI, as well as error correlate detection during control of more complex BCI effectors using multiple degrees of freedom.

AUTHOR CONTRIBUTIONS

VR and MS performed the analyses and wrote the manuscript. VR and TA designed the task. ALB and TA provided input and mentorship through the analysis and writing. TC collected the data.

ACKNOWLEDGMENTS

REFERENCES

Benabid, A. L., Costecalde, T., Eliseyev, A., Charvet, G., Verney, A., Karakas, S., … Chabardes, S. (2019). An exoskeleton controlled by an epidural wireless brain–machine interface in a tetraplegic patient: A proof-of-concept demonstration. *The Lancet Neurology*. https://doi.org/10.1016/S1474-4422(19)30321-7

Blumberg, J., Rickert, J., Waldert, S., Schulze-Bonhage, A., Aertsen, A., & Mehring, C. (2007). Adaptive Classification for Brain Computer Interfaces. *2007 29th Annual International Conference of the IEEE Engineering in Medicine and Biology Society*, 2536–2539. https://doi.org/10.1109/IEMBS.2007.4352845

Chavarriaga, R., Iturrate, I., & Millan, J. del R. (2016, May 30). *Robust, accurate spelling based on error-related potentials.*

Chavarriaga, R., & Millan, J. d R. (2010). Learning From EEG Error-Related Potentials in Noninvasive Brain-Computer Interfaces. *IEEE Transactions on Neural Systems and Rehabilitation Engineering*, *18*(4), 381–388. https://doi.org/10.1109/TNSRE.2010.2053387

Chavarriaga, R., Sobolewski, A., & Millan, J. d R. (2014). Errare machinale est: The use of error-related potentials in brain-machine interfaces. *Frontiers in Neuroscience*, *8*. https://doi.org/10.3389/fnins.2014.00208

Eliseyev, A., Auboiroux, V., Costecalde, T., Langar, L., Charvet, G., Mestais, C., … Benabid, A.-L. (2017). Recursive Exponentially Weighted N-way Partial Least Squares Regression with Recursive-Validation of Hyper-Parameters in Brain-Computer Interface Applications. *Scientific Reports*, *7*(1), 1–15. https://doi.org/10.1038/s41598-017-16579-9

Even-Chen, N., Stavisky, S. D., Pandarinath, C., Nuyujukian, P., Blabe, C. H., Hochberg, L. R., … Shenoy, K. V. (2018). Feasibility of Automatic Error Detect-and-Undo System in Human Intracortical Brain–Computer Interfaces. *IEEE Transactions on Biomedical Engineering*, *65*(8), 1771–1784. https://doi.org/10.1109/TBME.2017.2776204

Falkenstein, M., Hohnsbein, J., Hoormann, J., & Blanke, L. (1991). Effects of crossmodal divided attention on late ERP components. II. Error processing in choice reaction tasks. *Electroencephalography and Clinical Neurophysiology*, *78*(6), 447–455. https://doi.org/10.1016/0013-4694(91)90062-9

Ferrez, P. W., & del R. Millan, J. (2008). Error-Related EEG Potentials Generated During Simulated Brain–Computer Interaction. *IEEE Transactions on Biomedical Engineering*, *55*(3), 923–929. https://doi.org/10.1109/TBME.2007.908083

Inoue, M., Uchimura, M., & Kitazawa, S. (2016). Error Signals in Motor Cortices Drive Adaptation in Reaching. *Neuron*, *90*(5), 1114–1126. https://doi.org/10.1016/j.neuron.2016.04.029

Iturrate, I., Chavarriaga, R., Montesano, L., Minguez, J., & Millán, J. d R. (2012). Latency correction of error potentials between different experiments reduces calibration time for single-trial classification. *2012 Annual International Conference of the IEEE Engineering in Medicine and Biology Society*, 3288–3291. https://doi.org/10.1109/EMBC.2012.6346667

Koelewijn, T., van Schie, H. T., Bekkering, H., Oostenveld, R., & Jensen, O. (2008). Motor-cortical beta oscillations are modulated by correctness of observed action. *NeuroImage*, *40*(2), 767–775. https://doi.org/10.1016/j.neuroimage.2007.12.018

Lotte, F., Bougrain, L., Cichocki, A., Clerc, M., Congedo, M., Rakotomamonjy, A., & Yger, F. (2018). A review of classification algorithms for EEG-based brain-computer interfaces: A 10 year update. *Journal of

Neural Engineering, *15*(3). Scopus. https://doi.org/10.1088/1741-2552/aab2f2

Mestais, C. S., Charvet, G., Sauter-Starace, F., Foerster, M., Ratel, D., & Benabid, A. L. (2015). WIMAGINE: Wireless 64-Channel ECoG Recording Implant for Long Term Clinical Applications. *IEEE Transactions on Neural Systems and Rehabilitation Engineering*, *23*(1), 10–21. https://doi.org/10.1109/TNSRE.2014.2333541

Milekovic, T., Ball, T., Schulze-Bonhage, A., Aertsen, A., & Mehring, C. (2012). Error-related electrocorticographic activity in humans during continuous movements. *Journal of Neural Engineering*, *9*(2), 026007. https://doi.org/10.1088/1741-2560/9/2/026007

Milekovic, T., Ball, T., Schulze-Bonhage, A., Aertsen, A., & Mehring, C. (2013). Detection of Error Related Neuronal Responses Recorded by Electrocorticography in Humans during Continuous Movements. *PLOS ONE*, *8*(2), e55235. https://doi.org/10.1371/journal.pone.0055235

Parra, L. C., Spence, C. D., Gerson, A. D., & Sajda, P. (2003). Response error correction-a demonstration of improved human-machine performance using real-time EEG monitoring. *IEEE Transactions on Neural Systems and Rehabilitation Engineering*, *11*(2), 173–177. https://doi.org/10.1109/TNSRE.2003.814446

Schalk, G., Wolpaw, J. R., McFarland, D. J., & Pfurtscheller, G. (2000). EEG-based communication: Presence of an error potential. *Clinical Neurophysiology: Official Journal of the International Federation of Clinical Neurophysiology*, *111*(12), 2138–2144. https://doi.org/10.1016/s1388-2457(00)00457-0

Schie, H. T. van, Mars, R. B., Coles, M. G. H., & Bekkering, H. (2004). Modulation of activity in medial frontal and motor cortices during error observation. *Nature Neuroscience*, *7*(5), 549–554. https://doi.org/10.1038/nn1239

Spüler, M., Rosenstiel, W., & Bogdan, M. (2012). Online Adaptation of a c-VEP Brain-Computer Interface(BCI) Based on Error-Related Potentials and Unsupervised Learning. *PLoS ONE*, *7*(12), e51077. https://doi.org/10.1371/journal.pone.0051077

Völker, M., Fiederer, L. D. J., Berberich, S., Hammer, J., Behncke, J., Kršek, P., … Ball, T. (2018). The dynamics of error processing in the human brain as reflected by high-gamma activity in noninvasive and intracranial EEG. *NeuroImage*, *173*, 564–579. https://doi.org/10.1016/j.neuroimage.2018.01.059

Wilson, N. R., Sarma, D., Wander, J. D., Weaver, K. E., Ojemann, J. G., & Rao, R. P. N. (2019). Cortical Topography of Error-Related High-Frequency Potentials During Erroneous Control in a Continuous Control Brain–Computer Interface. *Frontiers in Neuroscience*, *13*, 502. https://doi.org/10.3389/fnins.2019.00502

Wodlinger, B., Downey, J. E., Tyler-Kabara, E. C., Schwartz, A. B., Boninger, M. L., & Collinger, J. L. (2014). Ten-dimensional anthropomorphic arm control

in a human brain-machine interface: Difficulties, solutions, and limitations. *Journal of Neural Engineering*, *12*(1), 016011. https://doi.org/10.1088/1741-2560/12/1/016011

Yeung, N., Holroyd, C., & Cohen, J. (2005, May). *ERP correlates of feedback and reward processing in the presence and absence of response choice*. Cerebral Cortex (New York, N.Y. : 1991). https://doi.org/10.1093/cercor/bhh153